ISSN 1995-0780, Nanotechnologies in Russia, 2008, Vol. 3, Nos. 11–12, pp. 734–742. © Pleiades Publishing, Ltd., 2008.
Original Russian Text © V.V. Lepov, A.M. Ivanov, B.A. Loginov, V.A. Bespalov, V.S. Achikasova, R.R. Zakirov, V.B. Loginov, 2008, published in Rossiiskie nanotekhnologii, 2008, Vol. 3, Nos. 11–12.

EXPERIMENT

The Mechanism of Nanostructured Steel Fracture at Low Temperatures

V. V. Lepov[a], A. M. Ivanov[a], B. A. Loginov[b], V. A. Bespalov[b], V. S. Achikasova[a], R. R. Zakirov[c], and V. B. Loginov[c]

[a] *Institute of Physical-Technical Problems of the North, Russian Academy of Sciences, ul. Oktyabr'skaya 1, Yakutsk, 6777980 Russia*
[b] *Moscow Institute of Electronic Technology (Technical University), Proezd 4806 5, Zelenograd, Moscow, 124498 Russia*
[c] *Moscow Engineering Physics Institute (State University) (MEPI), Kashirskoye Shosse 31, Moscow, 115409 Russia*
e-mail: lepov@iptpn.ysn.ru
logi@miee.ru

Received June 2, 2008

Abstract—Microstructural aspects of deformation and fracture of steel which is nanostructured using the technique of equal-channel angular pressing and thermal processing at low temperature (–60°C) are considered in the paper. The methods of optical and atomic-force microscopy are used to investigate deformation surfaces. The fracture character change (from a brittle cleavage to a ductile shear) at low temperatures is shown to be associated, on the one hand, with a fuzzing of grain boundaries during pressing with solid structural phases and, on the other hand, by the replacement of the prevalent plastic deformation carriers.

DOI: 10.1134/S1995078008110116

INTRODUCTION

A new spectrum of the research aimed at obtaining nanostructured and ultrafine–grained materials and at analyzing their applicability in conditions of the North allows solving the problem of brittle fracture at a new level, to study the effects of grain boundaries on structural degradation at low temperatures, and to investigate possible manifestations of ductile-brittle transitions in such materials.

To obtain ultrafine-grained materials we used a technique of intensive plastic deformation, namely, equal-channel angular pressing (ECAP) [1]. Multiple (multipass) application of ECAP accompanied by thermal processing allows improving a complex of mechanical properties of the majority of metals, iron-based ones included [2], as well as their cold resistance, determined by the amount of the fracture specific energy during impact bending tests (i.e., by the impact elasticity) [3]. However, microscopic mechanisms of brittle fracture and peculiarities of damage accumulation in such materials are not adequately studied as yet.

The technique of tunneling scanning microscopy [4] makes it possible to study the structure of material surfaces at a high nanometric resolution. A degree of roughness points to the surface maturity: the more mature the surface, the greater the roughness. The efficiency of scanning atomic-force and tunneling microscopy for studying surface defects and for performing monitoring in the case of refining novel surface modification technologies is well-known [5].

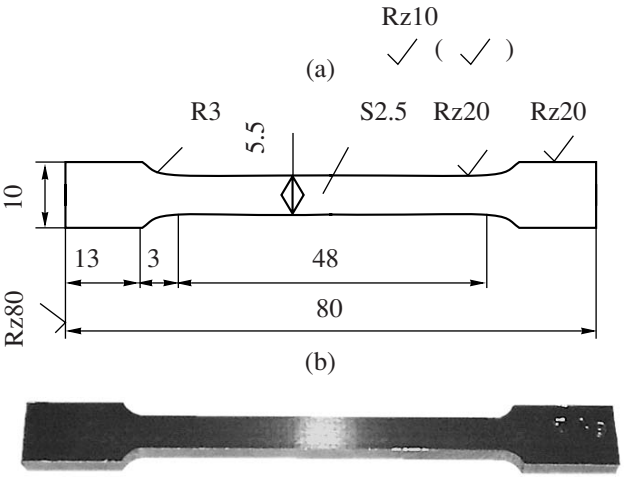

Fig. 1. Main sizes (a) and an overall view (b) of the samples to be stretched.

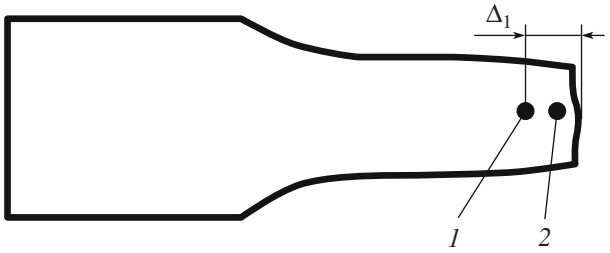

Fig. 2. Diagram of scanning regions selection in a deformed sample.

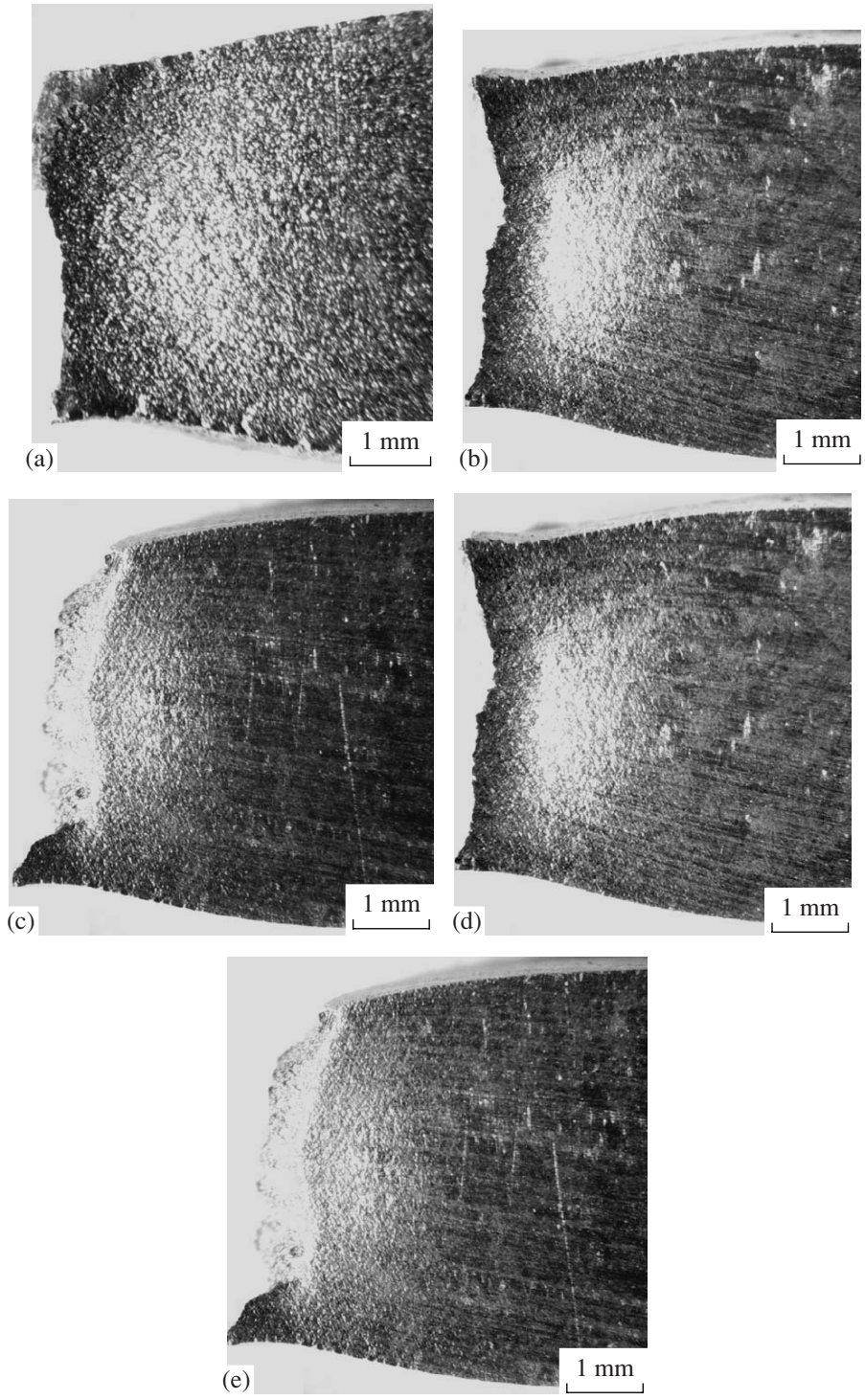

Fig. 3. Photographs of the sample fracture region (ECAP along the C path at 400°C): (a) from the source material tested at 20°C; (b) from the material subjected to 2 ECAP passes tested at 20°C; (c) from the material subjected to 2 ECAP passes tested at –60°C; (d) from the material subjected to 8 ECAP passes tested at 20°C; (e) from the material subjected to 8 ECAP passes tested at –60°C.

Due to high accuracy in determining surface profile heights, the techniques of scanning atomic-force and tunneling spectroscopy are the most appropriate for quantitative studies of the surface geometry of fractures and specially prepared microstructures. The atomic-force technique which is insensitive to non–conducting oxide film on a metal surface is the most suitable (from the two mentioned) for studying steel samples. In addition to a three-dimensional surface image, the technique allows getting a profilogram, thus making it pos-

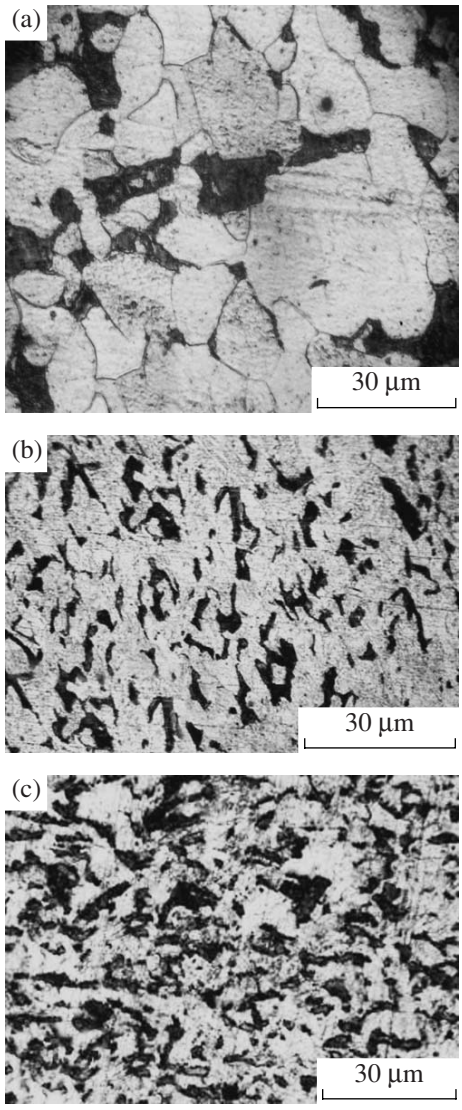

Fig. 4. Photographs of microstructures obtained with the technique of optical metallography: (a) the source material; (b) after 2 ECAL passes; (c) after 4 ECAP passes.

sible to quantitatively evaluate the surface geometry and to calculate, e.g., an average size of metal film crystallites [6], to determine the sizes of Widmanstatten ferrite plates and a deformation profile [7], and to reveal the mechanism of hydrogen embrittlement [8]. However, there are still very few papers which study nanostructured construction materials using scanning atomic-force and tunneling microscopy.

In the present paper the technique of scanning atomic-force microscopy is applied to investigations of the morphology of surface stretching deformations of samples fractured at different temperatures. At that, microstructure peculiarities of damage accumulation and the character of nanostructured steel fractures at low temperatures were revealed.

RESEARCH TECHNIQUE

The deformation surface was studied using flat samples made of St3sp steel in the initial (normalized) state and after its ECAP processing along the C path (after each pass a billet rotated by 180° around its longitudinal axis), the number of passes being 2 and 8. The sizes and the form of the stretched samples are shown in Fig. 1, whereas test results are tabulated in table.

The regions localized in the vicinity of the sample neck (fracture) at different distances from the fracture point were studied using scanning atomic-force microscopy with an aim to reveal micromechanisms and plastic deformation carriers. The resolution achieved when this technique was implemented with the SMM-200 microscope (manufactured by Proton-MIEE, Zelenograd), the samples being studied in the air, was not worse than 2–3 nm. The samples were cut with a diamond disc with water cooling till the longitudinal size was 6 mm, their surface was etched with orthophosphoric acid not more than 0.2 μm deep to reveal phase boundaries, the oxidized layer was removed, and chemical passivation was performed.

Figure 2 shows the diagram of the selection of scanning regions in a plastically deformed sample area, whereas photographs of sample surfaces in the fracture region are given in Fig. 3. The level of plastic deformation ε_1 in region 1 will be smaller that that of ε_2 in region 2 (Fig. 2). The extent of residual plastic deformation will be approximately determined by the necking value. Thus, the surface morphology in region 1, which is Δ_1–away from the fracture point, will show the stage of defectiveness evolution, corresponding to an earlier stage of plastic yielding. For investigation pur-

The data obtained during mechanical tensile tests for St3sp steel samples sunjected to ECAP

State of material	Average grain dimension d_m, μm	Microstrength H_V, MPa	Yield strength σ_T, MPa		Ultimate strength σ_B, MPa		Relative elongation during fracture, δ, %	
			20°C	–60°C	20°C	–60°C	20°C	–60°C
Initial	18.5	1370	324.4	–	498.4	–	14.5	–
2ECAP passes	10.5	2500	750	825	791	863.5	4.95	8.95
8ECAP passes	6.5	2910	830	915	844	921.5	5.36	5.10

Note: The tabulated values for σ_T, σ_B and δ are given for the samples whose deformation surfaces were studied directly, whereas the values for d_m and H_V are the ones averaged for all the group of the tested samples.

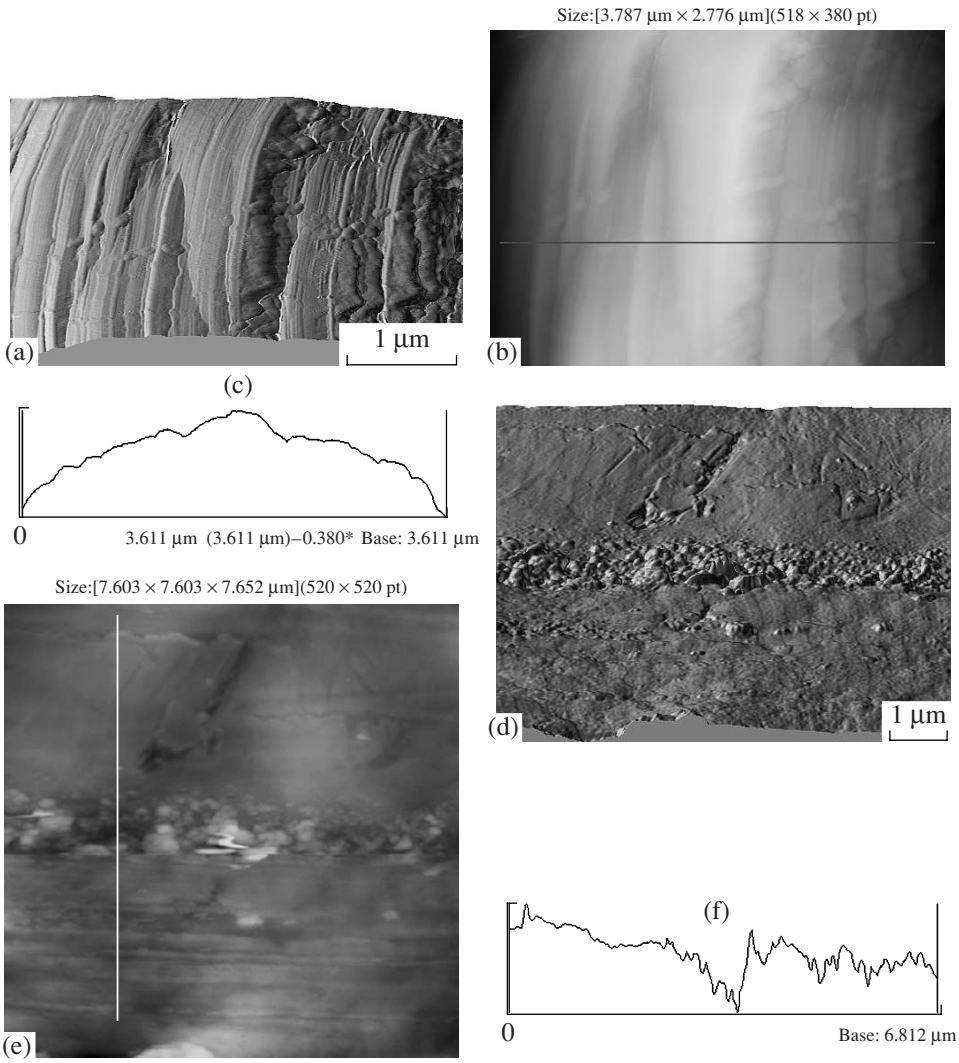

Fig. 5. Three- and two-dimensional images of the deformation surface and geometry of the sample made of the source material 500 μm (a–c) and 3.0 mm (d–f) away from the fracture point: (a), (d) a three-dimensional image; (b), (d) a two-dimensional image; (c), (f) geometry of the surface corresponding to a two-dimensional image.

poses the distance Δ was chosen as 200 and 500 μm, and 1, 2 and 3 mm, but the present paper considers the most informative surface images for the regions, which were 500 μm and 3 mm away from the fracture. The size of the scanning area was 8×8 and 4×4 μm^2.

The microstructure photographs, obtained by the optical metallography technique, are shown in Fig. 4. The photographs showing steel microstructure after ECAP (Figs. 4b, 4c) reveal texture formation and orientation of ferrite phases along the direction of pressing. After 8 ECAP passes (Fig. 4c) the grain shape becomes difficult to be determined, whereas its average size is calculated using the method of random secants.

STUDY OF DEFORMATION SURFACES WITH ATOMIC-FORCE SPECTROSCOPY

Due to the fact that we studied 5 sample surfaces (in the initial state (after hot rolling) and after 2 and 8 ECAP passes along the C path) at 20°C and –60°C, the results are given as compared to each studied region. For the region that is 500 μm away, the level of plastic deformation is critical for such type of loading and corresponds to the maximum dislocation densities. The region that is 3 mm away from the fracture is the region of moderate plastic deformation, its value making approximately 40% of the critical one. Thus, the comparison of surface morphologies and characteristic profiles of these regions, obtained with a high nanometric resolution, will allow for the materials after ECAP to reveal key differences in the realization of damage accumulation mechanisms at different stages of plastic deformation development at different test temperatures.

Figure 5 shows three- and two-dimensional images of steel surfaces with the initial structure 500 μm and 3 mm away from the fracture, as well as nanometric profiles of these regions. The maximum height of the region profile 500 μm away from the fracture is

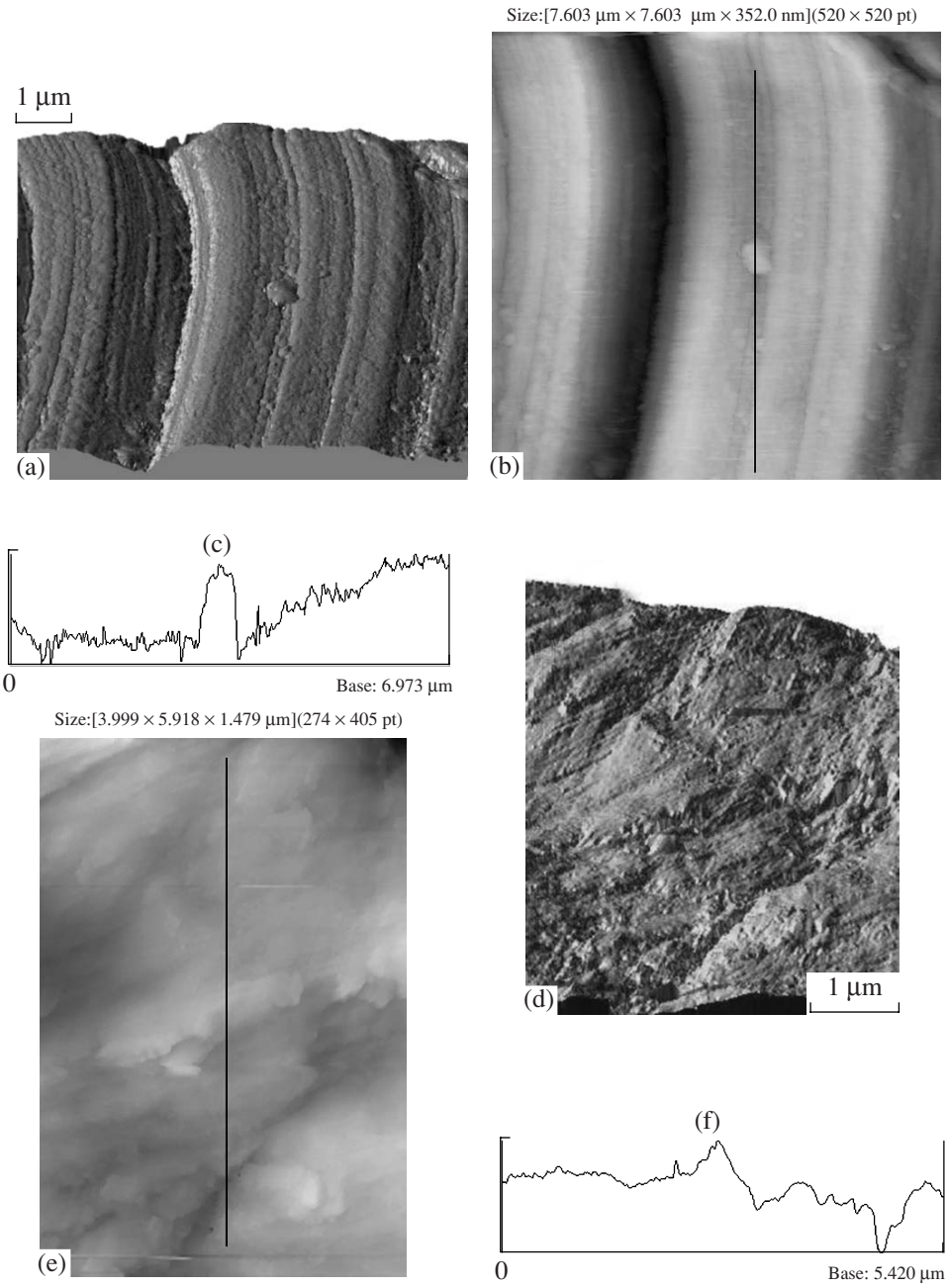

Fig. 6. Three- and two-dimensional images of the deformation surface and geometry of the sample made of the material subjected to 2 ECAP passes (500 μm away from the fracture point) and tested at: (a), (b), (c) 20°C; (d), (e), (f) –60°C.

300 nm; 3 mm away, 215 nm. The images reveal a grained structure of the source material in spite of smoothened deformation geometry near the fracture (500 μm away). The deformation surface geometry 3mm away from the fracture clearly reflects a subgrained structure and phase boundaries (Fig. 5d), some twin slip lines entering the surface.

Figure 6 shows the images of the deformation surface and region profiles 500 μm away from the fracture in the samples made of the material subjected to 2 ECAP passes and tested at room (a–c) and low (d–f) temperatures. The profile heights are 88 and 414 nm for the tests and room and low temperatures, respectively. Such a large spread of profile heights characterizes the differences in the fracture process energy consumption, because at small distances from the fracture the deformation level is close to that critical for the given material. At room temperature the deformation geometry of plastic deformation is smoothened and is similar to that for the sample made of the source material, though the grained structure is no longer noticeable. At low temperatures the deformation geometry is clearly separated

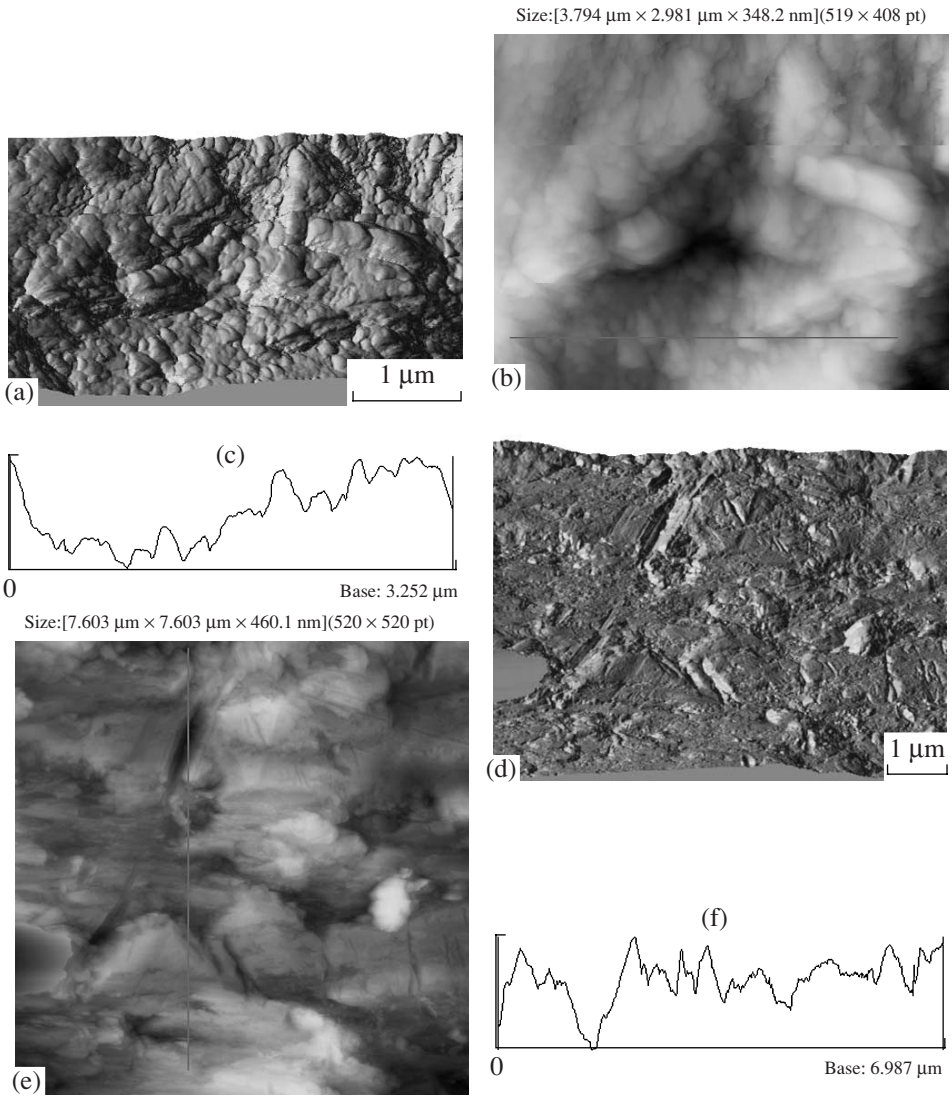

Fig. 7. Three- and two-dimensional images of the deformation surface and geometry of the sample made of the material subjected to 2 ECAP passes (3 mm away from the fracture point) and tested at: (a), (b), (c) 20°C; (d), (e), (f) –60°C.

by multiple intragranular crystallite inclusions, which enter the surface. The size of these structures is nearly 200–300 nm, and the shear lines completely disappear.

Three- and two-dimensional images of the deformation surface and the profile of the regions 3 mm away from the fracture for the samples made of the material which was subjected to two ECAP passes and tested at room (a–c) and low (–60°C) temperatures (d–e) are shown in Fig. 7. The profile heights are 125 and 250 nm for tests at room and low temperatures, respectively, which correspond to a medium level of plastic deformation for these samples (Figs. 3b, 3c). Here, the change of the plastic deformation character should be taken into account; a rough shear mechanism with splitting and microcracks formation prevails.

Figure 8 shows the images of the deformation surface 500 μm away from the fracture in the samples made of the material subjected to 8 ECAP passes and tested at room and low (–60°C) temperatures. The spreads of profile heights are 66 and 112 nm for room and low test temperature, respectively. Here, we observe lineage deformation structures corresponding to the pressing direction. Shear lines due to twinning are completely absent.

Three- and two-dimensional images of the deformation surface and the profile of the regions 3.0 mm away from the fracture in the samples made of the material, which was subjected to 8 ECAP passes and tested at room and low temperatures, are shown in Fig. 9. The profiles have a similar height spread, namely, 127 nm and 120 nm for room and low test temperature, respectively. Lineage deformation structures corresponding to the pressing directions are preserved here as well, and are more noticeable in the case of room temperature deformation. At low test temperatures we also observe fractures, but they are laminated, contrary to microc-

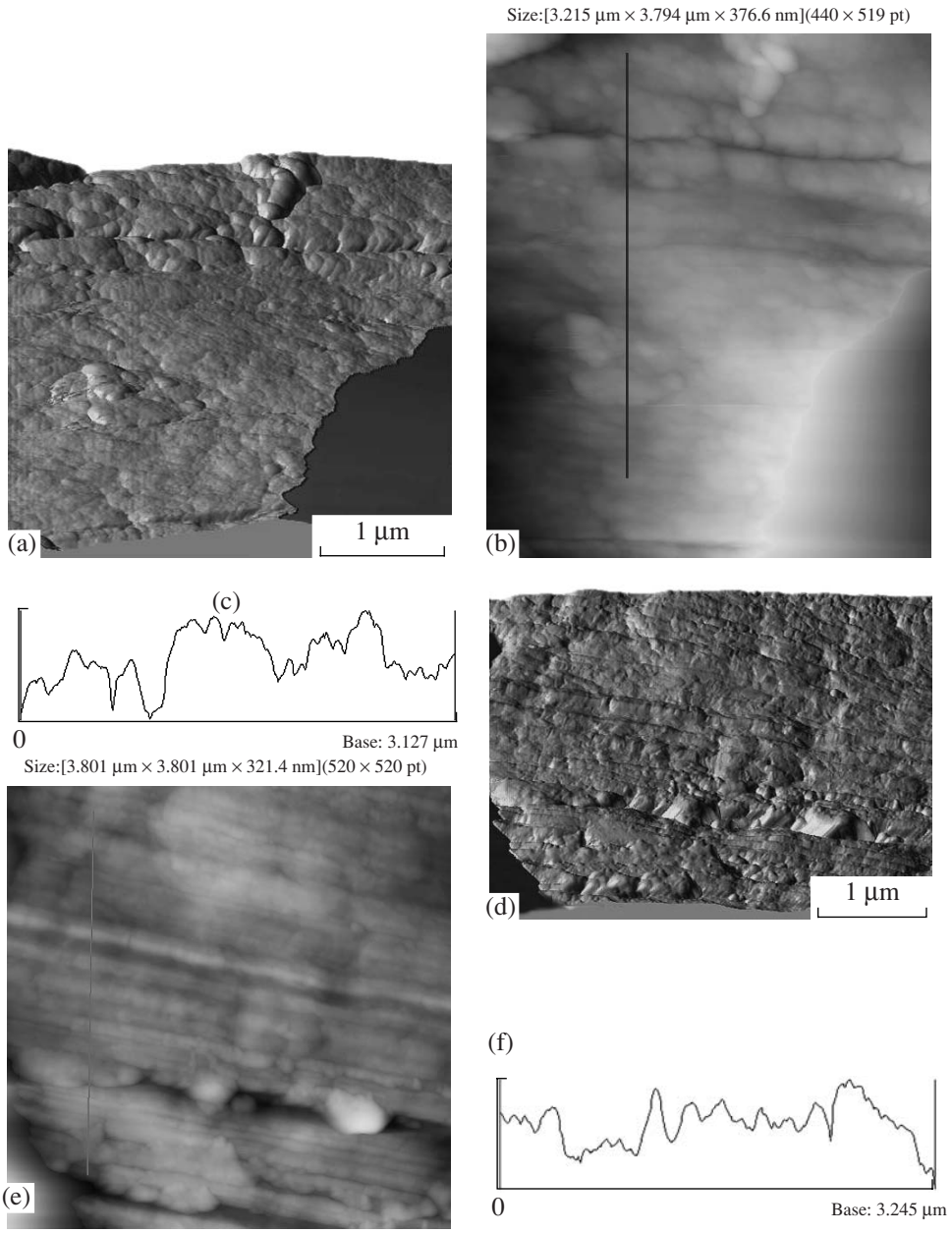

Fig. 8. Three- and two-dimensional images of the deformation surface and geometry of the sample made of the material subjected to 8 ECAP passes (500 μm away from the fracture point) and tested at: (a), (b), (c) 20°C; (d), (e), (f) –60°C.

racks in the steel subjected to two ECAP passes. The observable deformation structures are amorphous phase boundaries and their sizes are less than 50–100 nm, shear lines being absent as well.

RESULTS AND DISCUSSION

It is known that such microstructure parameters as the size of a grain or subgrain; the quantity, the distribution and the morphology of solid disperse particles (carbides) and structural components; as well as the nature and the chemical composition of a solid solution determine steel strength and resistance to brittle fracture.

For nanostructured steel we cannot apply the Hall-Petch dependence for the yield stress σ_T [9]:

$$\sigma_T = \sigma_i + K_T d^{-n}, \quad (1)$$

because in the materials subjected to only 2 ECAP passes along the C path only small–angle grain boundaries are mainly formed [2, 10], and the exponent n will be close to a unity, whereas in cases of 8 passes of such "warm" pressing the equilibrium large-angle boundaries are formed [10], and $n \sim 0.5$. In Eq. (1) σ_i is the friction stress, hindering the dislocation motion, which characterizes the strength of the metal matrix without taking into account the boundary effect, and the second

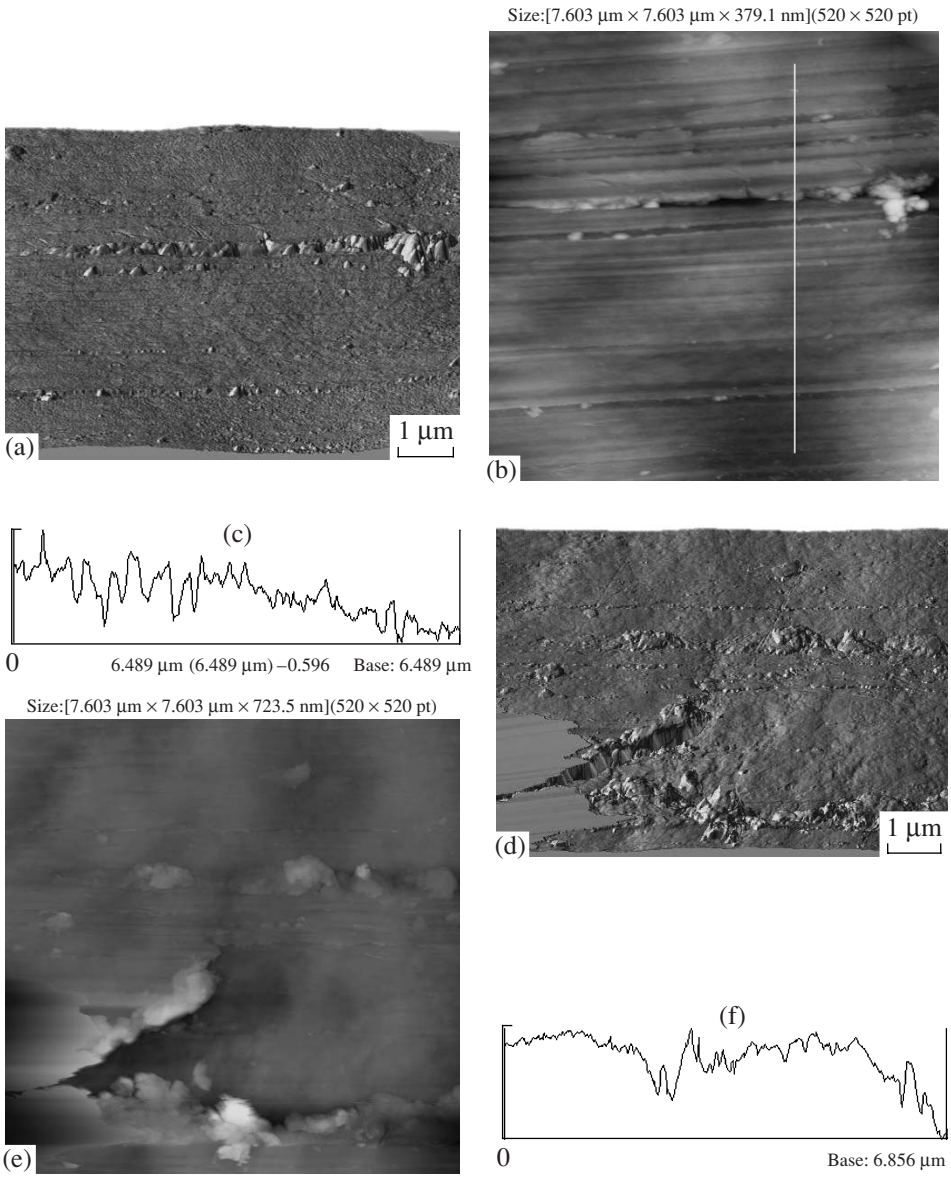

Fig. 9. Three- and two-dimensional images of the deformation surface and geometry of the sample made of the material subjected to 8 ECAP passes (3 mm away from the fracture point) and tested at: (a), (b), (c) 20°C; (d), (e), (f) –60°C.

term determines the boundary and subboundary contribution into strengthening. Here K_T is the constant which depends on the metal composition and the structure of the grain boundaries, and d is the average size of a grain or a subgrain. In some cases d is considered an interparticle distance as well [11]. It is the formation of an equilibrium grain structure with large-angle boundaries that sets conditions for increased indices of impact strength of nanostructured steels at low temperature tests [3].

The present paper studies steel that is characterized by the structure of grains with fragment sizes that provides for a unique increase of mechanical properties. In spite of the fact that after 8 ECAP passes the average size of grains in St3sp steel, determined with a metallographic method, is nearly 6.5 μm, the sizes of fragments determined using transmission electron microscopy (TEM) are less than 1 μm [12]. The data obtained, in particular, with atomic-force microscopy of deformation surfaces point to smaller fragment sizes (less than 100 nm).

Thus, in the deformation surface geometry of samples subjected to 8 ECAP passes and tested at 20°C and –60°C we observe lineage deformation structures (Figs. 9a, 9d) with carrier sizes of nearly 20 nm (Figs. 9c, 9f).

The surface geometry of samples made of the material subjected to 2 ECAP passes are non-uniform and demonstrate increased roughness which is characterized by grain splitting into small subgrains with different hardness. Dislocations and shear lines turn from clearly noticeable isolated formations into multiple

phase boundaries which are practically completely extruded from the grain body.

Based on the obtained images and surface geometries we can see that the key distinction in the fracture character of nanostructured steels subjected to 2 and 8 ECAP cycles at low test temperatures lies in a more ductile character of fracture, a uniform and a developed roughness with a high energy dissipation that, in its turn, is associated with a greater equilibrium, and finer material structure.

Note that in the samples made of nanostructured St3sp steel subjected to a breaking test, fuzzing of the grain boundaries due to the interaction of soft and solid phases was revealed. Thus, if on the deformation surface of the source material samples we can clearly see grain boundaries (Figs. 5a, 5d), in the samples made of the material subjected to 2 and 8 ECAP passes these boundaries are either not noticeable against a background of deformation structures (Figs. 6a, 6d; 7a, 7d) or strongly fuzzed (Figs. 8a, 8d; 9a, 9d). Also note the changes in the character of plastic deformation in the samples subjected to 8 ECAP passes (Figs. 8, 9) which hinder the concentration of fractures typical for the samples made of the material subjected to 2 passes (Figs. 6, 7). The traces of slippage of dislocation nature, inherent to the source material, do not show up on the body of fine grains with a lineage structure (Figs. 5d, 5e).

A coarser shear character of the deformation surface near the fracture surface is characteristic for low-temperature tests of the steel with the initial structure [3] and after 2 ECAP passes (Figs. 7a, 7d). For nanostructured steels this process is smoothened and has a ductile-brittle character (Figs. 8a–9d), which shifts the temperature of a ductile-brittle transition for all the items to the range of lower temperatures.

In confirmation of data obtained, some authors [13, 14] who studied the mechanisms of deformation of ultrafine-grain alloys after several ECAP passes with the technique of transmission electron and X-ray microscopy revealed that dislocation slipping becomes the main deformation mechanism in such materials as compared to twinning.

Based on the performed microstructure studies, it is evident that the production of a more strengthened and non-uniform structure prior to ECAP using thermal processing or other techniques must help obtain better mechanical characteristics and increase fracture energy consumption, in the case of the included low-temperature tests.

ACKNOWLEDGMENTS

This study was performed within the framework of the Federal Target Program (State contract no. 02.513.11.3056 of March 22, 2007), supported by ISTC (project no. 3399) and, in part, by the Program for Basic Research of RAS Presidium (project no. 8.5), specialized RAS departments (project no. 4.11.1 of OEMMPU RAS) and the Russian Foundation for Basic Research, project nos. 05-08-33649 and 06-01-96018-p-vostok.

REFERENCES

1. V. M. Segal, V. I. Reznikov, V. I. Kopylov, et al., *Processes of Plastic Structure Formation in Metals* (Navuka i Tekhnika, Minsk, 1994) [in Russian].
2. R. Z. Valiev and I. V. Aleksandrov, *Nanostructured Materials Produced under Severe Plastic Deformation* (Logos, Moscow, 2000) [in Russian].
3. M. Z. Borisova, S. P. Yakovleva, and A. M. Ivanov, "Equal Channel Angular Pressing and Its Effect on Structure and Properties of the Constructional Steel St3," Solid State Phenom. **114**, 97–101 (2006).
4. G. Binnig, H. Rohrer, Ch. Gerber, and E. Weibel, "Surface Studies by Scanning Tunneling Microscopy," Phys. Rev. Lett. **49**, 57–61 (1982).
5. A. L. Suvorov, Yu. N. Cheblukov, N. E. Lazarev, et al., "Field Ion and Scanning Tunnel Microscopy Studies of Surface and Bulk Defects in Carbon and Silicon," Zh. Tekh. Fiz. **70** (3), 56–61 (2000) [Tech. Phys. **45** (3), 343 (2000)].
6. Yu. A. Bykov, S. D. Karpukhin, and E. I. Gazukina, "On Some Special Features of the Structure and Properties of Metallic "Thin" Films," Metalloved. Term. Obrab. Met., No. 6, 45–47 (2000) [Met. Sci. Heat Treat. **42** (6), 250–252 (2000)].
7. X. Bo, H. Fang, and J. Wang, "Investigation of Surface Relief Accompanying Widmanstatten Ferrite Formation by Scanning Tunneling Microscopy," Scr. Mater. **39** (2), 247–252 (1998).
8. E. A. Arkhangel'skaya, V. V. Lepov, and V. P. Larionov, "The Role of Defects in the Development of Decelerated Destruction of a Damaged Medium under the Action of Hydrogen," Materialovedenie, No. 8, 7–10 (2003).
9. H. Liebowitz, *Fracture: An Advanced Treatise*, Vol. 6: *Fracture of Metals* (Metallurgiya, Moscow, 1996; Academic, New York, 1969).
10. P. D. Gorelik, S. V. Dobatkin, and L. M. Kaputkina, *Recrystallization of Metals and Alloys*, 3rd ed. (Moscow Institute of Steel and Alloys, Moscow, 2005) [in Russian].
11. P. D. Odesskii, I. I. Vedyakov, and V. M. Gorpinichenko, *Prevention of Brittle Fracture of Metalwork Structural Constructions* (SP Intermet Inzhiniring, Moscow, 1998) [in Russian].
12. G. I. Raab, A. M. Ivanov, D. V. Gunderov, et al., "Increase in the Strength and Cold Resistance of Structural Steels under Severe Plastic Deformation and Heat Treatment," in *Proceedings of the Second All-Russian Conference on Nanomaterials "NANO—2007" and the Fourth Russian–Belarusian Workshop "Nanostructured Materials—2007," Novosibirsk, Russia, March 13–16, 2007* (Institute of Solid-State Chemistry and Mechanochemistry, Siberian Branch, Russian Academy of Sciences, Novosibirsk, 2007), p. 390.
13. W. Q. Cao, S. H. Yu, Y. B. Chun, et al., "Deformation Mechanism of Zr702 Processed by Equal Channel Angular Pressing," Metall. Mater. Trans. A **38** (11), 2805–2814 (2007).
14. W. S. Choi, H. S. Ryoo, S. K. Hwang, et al., "Microstructure Evolution in Zr under Equal Channel Angular Pressing," Metall. Mater. Trans. A **33** (3), 973–980 (2002).